A viscoelastic sandwich beam finite element model

D.Sc. Flávio de Souza Barbosa[1], D.Sc. Michèle Cristina Resende Farage[2], Waldir Neme Felippe Filho[3], Eduardo da Silva Castro[4]

[1] *Universidade Federal de Juiz de Fora, Faculdade de Engenharia, Departamento de Estruturas, Juiz de Fora, Minas Gerais, Brasil*
[2] *Universidade Federal de Juiz de Fora, Faculdade de Engenharia,Departamento de Estruturas, Juiz de Fora, Minas Gerais, Brasil*
[3] *Universidade Federal de Juiz de Fora, Faculdade de Engenharia, Juiz de Fora, Minas Gerais, Brasil*
[4] *Universidade Federal de Juiz de Fora, Faculdade de Engenharia, Juiz de Fora, Minas Gerais, Brasil*

Resumo: Entre os sistemas de controle passivo para atenuação de vibrações em estruturas, aqueles que usam materiais visco-elásticos como núcleo dissipador de energia de vibração em vigas sanduíche são abordados neste trabalho. Apresenta-se um modelo numérico baseado numa formulação denominada GHM (Golla-Hughes Method) que simula o comportamento dinâmico de materiais visco-elásticos. Os parâmetros do GHM usados na caracterização do material visco-elástico foram determinados experimentalmente e um modelo de elemento finito sanduíche foi obtido e validado através de comparações entre resultados numéricos e experimentais, demonstrando um desempenho favorável do modelo proposto.

Palavras-chave: Materiais visco-elásticos; vigas sanduíche; atenuadores de vibração

Abstract: Among the passive control systems for attenuation of vibrations in structures, those that use viscoelastic materials as a damping core in laminated-plate-like components are focused herein. In the present work an assessment of a time domain formulation for numerical modeling of viscoelastic materials is made. This formulation, known as GHM (Golla-Hughes Method), is based on the viscoelastic Young's modulus representation in Laplace's domain. The GHM parameters used in the characterization of a viscoelastic material are experimentally determined. Finally, a sandwich finite element model obtained through GHM was validated by means of comparisons between numerical results and their experimental counterpart, demonstrating a favorable performance of this mathematical-numerical model.

Key-words: Viscoelastic materials; sandwich beams; passive damping

Introduction

The modeling of viscoelastic materials has two main applications: Firstly, the simulation of rheological problems. Normally, in this case, the inertial forces involved in the problem are not taken into account and this kind of analysis is known as quasi-static. The classic models of Maxwell, Voigt and Kelvin and references Beijer (2002) and Mesquita (2003) are typical examples of such models. Secondly, real dynamic problems involving viscoelastic materials have also been studied since the 50's in the works of Orbest (1952), Kelvin (1959) and Ross (1959). In general, these kind of models simulate the dynamic structural behavior of the viscoelastic material working as passive vibration control systems.

Vibration control systems assembled to structures, like the sandwich viscoelastic systems, have experienced a growth in practical applications due to some benefits related to cost-effectiveness and a high level of dynamic damping (Barbosa, 2000; Barbosa & Battista, 2000; Battista et al, 1998; Battista & Pfeil, 1999). One of the first large scale practical applications of sandwich viscoelastic elements in order to reduce vibrations was the World Trade Center, New York, USA. Some features of this kind of project were studied by Mahmoodi (1969) and Samali et al (1995). In Brazil, Battista et al (1998) developed dynamic tests in a prototype of Rio-Niterói bridge (Rio de Janeiro, Brazil) central spam, in 1:1 scale. This work consisted of a very comprehensive experimental program, including comparisons between the dynamic behavior of a concrete/steel deck and a sandwich (concrete/viscoelastic material/steel) deck, concluding that the sandwich deck has damping ratio considerable superior for high frequencies in this kind of application.

In order to model those systems, it is needed a formulation which takes into account the temperature and frequency dependence of the Young's modulus and the damping properties of the viscoelastic material.

When the relevant response of a sandwich viscoelastic system is framed in a short time interval, or in piecewise analysis, the temperature dependence may be ignored (Battista et al., 1998; Mahmoodi, 1969).

The consideration of frequency-dependent viscoelastic properties in time domain modelling is rather harder than in the frequency domain due to obvious reasons. References Kaliske & Rothert (1997), Qian & Demao (1990), Vasconcelos (2003a and 2003b), Yi et al. (1998) and Golla & Hughes (1985) present some alternatives to solve this problem.

The present work makes an assessment of a time domain formulation which adopts the frequency dependence of the viscoelastic properties in dynamic problems, having a short time interval of analysis. The employed formulation was implemented in a computational model within the framework of Finite Element (FE) method based on the Golla-Hughes Method (GHM) (Golla & Hughes, 1985).

The application of GHM relies on some parameters which characterizes the viscoelastic material. Such parameters are obtained herein, as described in section 3, via experimental tests.

As a numerical example, it is presented a sandwich FE model based on this formulation, which is capable to simulate the dynamic behavior of a experimentally tested sandwich beam. The theoretical formulation and the implemented solution method are thoroughly assessed by means of comparisons between numerical results and their experimental counterpart, demonstrating the favorable performance of this mathematical-numerical model.

1. The formulation of GHM

This section summarizes the GHM. Further details may be found in reference Golla & Hughes (1985).The complex Young's modulus may be expressed in Laplace domain as:

$$\varepsilon\left(s\right) = \varepsilon + h\left(s\right) \qquad (1)$$

where: □ is the elastic part of the complex modulus, $h(s)$ is the dissipation function associated to the damping and s is the Laplace variable. M. A. Biot (1955) (cited in Golla & Hughes, 1985) proposed a dissipation function as shown in Eq. (2).

$$h(s) = \frac{\alpha\left(s^2 + \beta s\right)}{s^2 + \beta s + \delta} \quad (2)$$

where: α , β and δ are obtained by curve fitting experimental curves.

The dynamic equilibrium equation for a single degree of freedom - dof - system in Laplace domain, considering null initial conditions and Eq. (1), is presented in Eq. (3).

$$\left[s^2\mathbf{M} + \varepsilon(s)\mathbf{K}\right]q(s) = \left[s^2\mathbf{M} + \varepsilon\mathbf{K} + h(s)\mathbf{K}\right]q(s) = f(s) \quad (3)$$

where: $\mathbf{M}$ is the mass of the system; $\mathbf{K}$ is part of the system stiffness which excludes the complex modulus expressed in Laplace domain; $q(s)$ is the dof and $f(s)$ is the excitation.

The aim of GHM is to express Eq. (3) in the time domain using a particular inverse Laplace transformation[1]. It may be proved that this particular transformation may be expressed in the form of Eq. (4).

$$\begin{bmatrix} \mathbf{M} & \mathbf{0} \\ \mathbf{0} & \alpha/\delta\mathbf{K} \end{bmatrix}\begin{Bmatrix} \ddot{q}(t) \\ \ddot{z}(t) \end{Bmatrix} + \begin{bmatrix} \mathbf{0} & \mathbf{0} \\ \mathbf{0} & \alpha\beta/\delta\mathbf{K} \end{bmatrix}\begin{Bmatrix} \dot{q}(t) \\ \dot{z}(t) \end{Bmatrix} + \begin{bmatrix} (\varepsilon+\alpha)\mathbf{K} & \alpha\mathbf{K} \\ \alpha\mathbf{K} & \alpha\mathbf{K} \end{bmatrix}\begin{Bmatrix} q(t) \\ z(t) \end{Bmatrix} = \begin{Bmatrix} f(t) \\ \mathbf{0} \end{Bmatrix} \quad (4)$$

where: t is the time variable, $z(t)$ is an additional dof called dissipation variable, with no physical meaning.

By using an analog process and some additional considerations described in Golla & Hughes (1985), it is possible to achieve the system of differential equations for a multi-dof finite element as shown in Eq. (5).

$$\mathbf{M}^{\upsilon}\begin{Bmatrix} \ddot{\mathbf{q}}(t) \\ \ddot{\mathbf{z}}(t) \end{Bmatrix} + \mathbf{C}^{\upsilon}\begin{Bmatrix} \dot{\mathbf{q}}(t) \\ \dot{\mathbf{z}}(t) \end{Bmatrix} + \mathbf{K}^{\upsilon}\begin{Bmatrix} \mathbf{q}(t) \\ \mathbf{z}(t) \end{Bmatrix} = \begin{Bmatrix} \mathbf{f}(t) \\ \mathbf{0} \end{Bmatrix} \quad (5)$$

where: $\mathbf{M}^{\upsilon} = \begin{bmatrix} \mathbf{M}^e & \mathbf{0} \\ \mathbf{0} & \alpha/\delta\mathbf{I} \end{bmatrix}$ (6), $\mathbf{C}^{\upsilon} = \begin{bmatrix} \mathbf{0} & \mathbf{0} \\ \mathbf{0} & \alpha\beta/\delta\mathbf{I} \end{bmatrix}$ (7) e $\mathbf{K}^{\upsilon} = \begin{bmatrix} (\varepsilon+\alpha)\mathbf{K}^e & \alpha\mathbf{R} \\ \alpha\mathbf{R}^T & \alpha\mathbf{I} \end{bmatrix}$ (8)

are, respectively, the mass, damping and stiffness matrices of the viscoelastic finite element, $\mathbf{M}^e$ is the finite element mass matrix considering an elastic system; $\mathbf{K}^e$ is the finite element

[1] Reference Barrett & Gotts, 2002, also deals with Laplace domain in order to simulate the dynamic behavior of viscoelastic systems.

stiffness matrix considering an elastic system and excluding the Young's modulus; $\mathbf{q}(t)$ and $\mathbf{z}(t)$ are, respectively, the displacement vectors of the real and dissipation dofs; $\mathbf{0}$ and $\mathbf{I}$ represents, respectively, the null and the identity matrix or vector; $\mathbf{f}(t)$ is the force vector; $\mathbf{R} = \mathbf{R}_d \mathbf{\Lambda}_d^{1/2}$; $\mathbf{R}_d$ is the matrix whose columns are the eigenvectors of $\mathbf{K}^e$ associated to the non-rigid body modes; and Λd is the diagonal matrix with the corresponding eigenvalues of $\mathbf{R}_d$.

The dimension of the viscoelastic matrices depends on the dimension of the corresponding elastic finite element and the number of dissipation variables. Each physical dof implies into one dissipation variable, although it is necessary to exclude those ones associated to rigid modes of $\mathbf{K}^e$. For example, for a plane quadrilateral linear finite element with 2 dof per node:

- Elastic dof: 4 nodes × 2 dof per node = 8 dof
- Dissipation variables: 8 - 3 (rigid modes: two translations and one rotation) = 5
- Dimension of the viscoelastic matrices: 8 + 5 = 13

Finally, GHM parameters (ε, α, β and δ) obtained from experimental data and Eqs. (6), (7) and (8) allow the determination of the viscoelastic finite element matrices for any kind of finite element model.

2. Determination of GHM parameters from experimental data

Equation 1 may also be expressed in the frequency domain, considering the dissipation function of Eq. (2), as shown in Eq. (9).

$$E^* = \varepsilon + \frac{\alpha\left(-\omega^2 + \iota\beta^2\omega\right)}{\omega^2 + \iota\beta\omega + \delta} \qquad (9)$$

where: E^* is the complex modulus expressed in the frequency domain; $\iota = \sqrt{-1}$; and ω is the frequency variable.

Commonly this complex modulus is divided into two parts:

- E': the real part, known as storage modulus
- η : the ratio between the imaginary and real parts, known as loss factor. Eqs (10) and (11) express, respectively, E' and η :

$$E' = \varepsilon + \frac{\alpha\omega^2\left(\omega^2 - \delta + \beta^2\right)}{\left(\delta - \omega^2\right)^2 + \beta^2\omega^2} \quad (10), \qquad \eta = \frac{\alpha\beta\omega\delta}{\left(\delta - \omega^2\right)^2 + \beta^2\omega^2}\frac{1}{E'} \quad (11)$$

The parameters ε, α, β and δ in Eqs. (10) and (11) are, in general, obtained by curve fitting of experimental results given in terms of E' and η. In this work experimental tests were developed in order to determine these parameters, by means of the sandwich beam technique (Nashif et al., 1985).

The experimental program concerned 6 beams of different lengths divided in 2 groups: a set of 3 simple beams, presented in Figure 1; and a set of 3 sandwich beams, presented in Figure 2. The simple set is composed by 3 elastic clumped-free aluminum beams having one single layer, and the sandwich set has tree viscoelastic sandwich clumped-free beams, with two layers of aluminum and the viscoelastic material in the core. For each set, the specimens lengths *L* were 50, 80 and 100 cm.

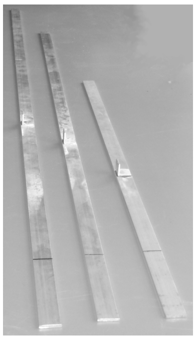
Figure 1: The Simple set.

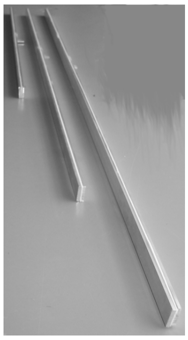
Figure 2: The Sandwich set.

Typical tests of a simple sample and a sandwich beam scheme are presented in Figures 3 and 4, respectively, showing the excited and the observed points valid for both sets.

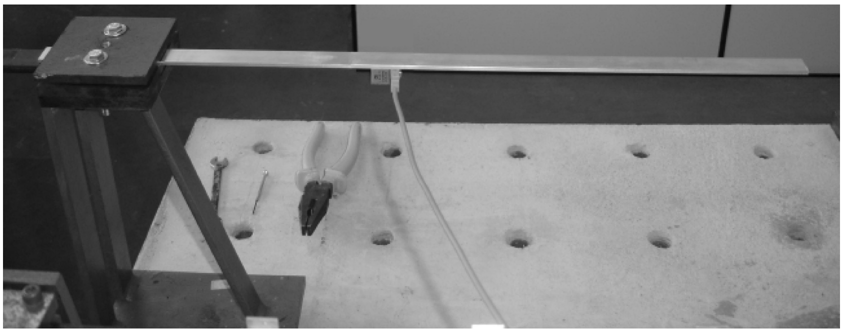
Figure 3: Photo of a typical simple specimen.

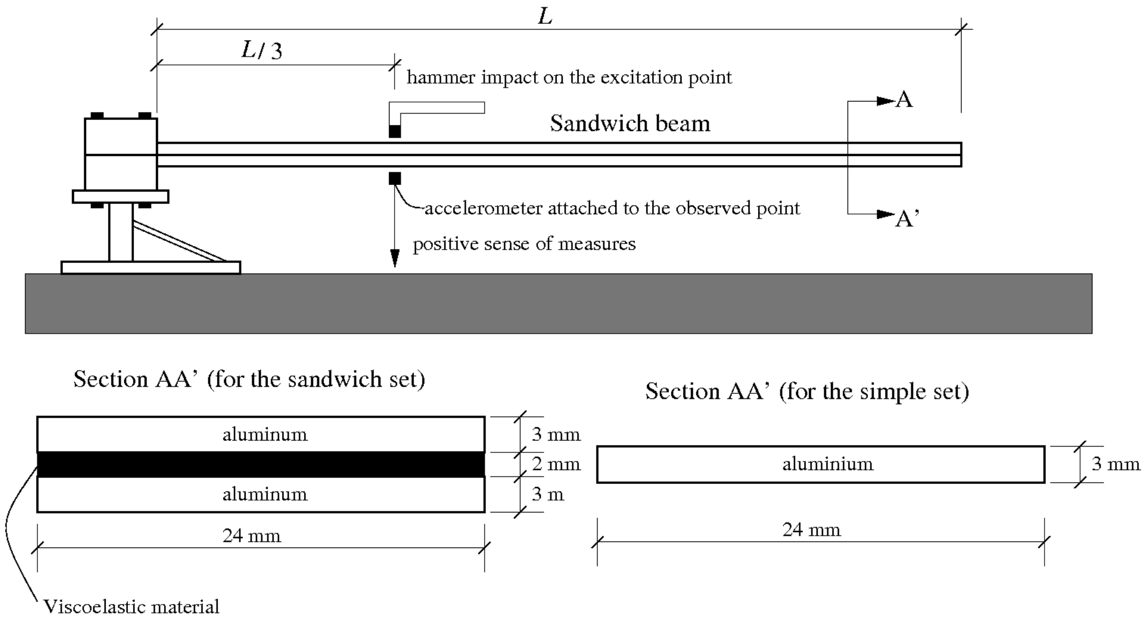

Figure 4: Typical schema of the tests.

The instrumentation consists of one accelerometer placed in the bottom of the samples, as indicated in Figure 3 and Figure 4. The main features of the used equipment and the data acquisition are: accelerometer model AS-GA Kyowa, rated capacity ±2g (safe over-loading 300%); acquisition system: Lynx ADS2000; frequency of acquisition 1000 Hz; low-pass filtering via hardware in 200 Hz; time of acquisition: 1 s.

Free vibration tests were performed, employing instantaneous hammer impact as excitation and figure 5 presents typical time responses for a simple sample and for a sandwich sample, both 100 cm long.

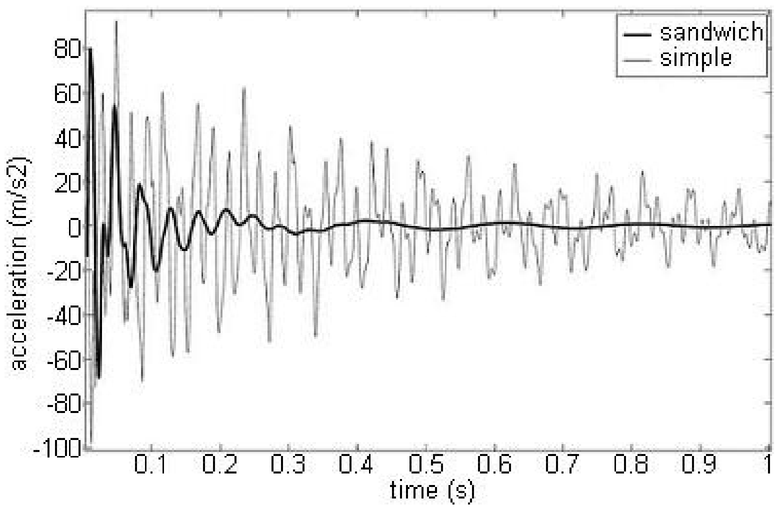

Figure 5: Typical time series for a simple and a sandwich specimen of 100 cm of length.

The experimental results in terms of the tree first natural frequencies, loss factor and standard deviations for the simple and the sandwich sets are presented in Tables 1 and 2, respectively. The modal identification was carried out using Random Decrement Method (Asmussen, 1998) and Ibrahim Time Domain Method (Ewins, 2000). Each sample was subjected to 4 tests, and modal identifications were carried out about 200 times, taking different parts of the responses.

Length (cm)	100 cm	80 cm	50 cm
f_1 (Hz) η_1	2.67 ± 0.10 0.0960 ± 0.0512	3.99 ± 0.05 0.0244 ± 0.0298	9.98 ± 0.01 0.0104 ± 0.002
f_2 (Hz) η_2	15.44 ± 0.03 0.0256 ± 0.0028	22.77 ± 0.04 0.0250 ± 0.0180	54.28 ± 0.09 0.0380 ± 0.0066
f_3 (Hz) η_3	42.93 ± 0.08 0.0210 ± 0.0206	63.62 ± 0.09 0.0258 ± 0.0180	157.72 ± 11.85 0.0730 ± 0.0356

Table 1: Summary of experimental results for the simple set.

Length (cm)	100 cm	80 cm	50 cm
f_1 (Hz) η_1	5.05 ± 0.02 0.1434 ± 0.0084	7.55 ± 0.03 0.1770 ± 0.0062	16.95 ± 0.04 0.1748 ± 0.0060
f_2 (Hz) η_2	24.54 ± 0.69 0.1508 ± 0.0374	37.13 ± 0.04 0.1768 ± 0.0058	79.33 ± 0.16 0.0765 ± 0.0102
f_3 (Hz) η_3	60.13 ± 0.31 0.1754 ± 0.0098	93.18 ± 2.41 0.078 ± 0.0668	184.44 ± 3.00 0.1350 ± 0.0142

Table 2: Summary of experimental results for the sandwich set.

Except for the third natural frequency of the 50 cm long simple sample, all the identified natural frequencies have standard deviation lower than 4%. The major part of natural frequencies had standard deviation inferior to 1%. In terms of damping modal identification, the standard deviations were more important, in accordance with the results presented in reference Cremona et al. (2003), although the mean values are not very different from those obtained by Faisca (1998).

By applying the equations presented in reference Nashif (1985), with the results of mean natural frequencies and mean loss factor obtained from the two tested sets, presented in Tables 1 and 2, it is possible to calculate E' and η for the viscoelastic material in the discrete values of natural frequencies of the sandwich set.

Figures 6 and 7 present, respectively, the storage modulus and the loss factor of the tested viscoelastic material. The solid lines in these figures indicate, respectively, E' (Pascal) and η obtained by curve fitting viscoelastic parameters ε , α , β and δ in Eqs. (10) and (11) via least square method to the discrete experimental points of E'. In this case, the curve fitted parameters of GHM where $\varepsilon = 0.58\,MPa$, $\alpha = 5.26\,MPa$, $\beta = 55.59 \cdot 10^6\ s^{-1}$ and $\delta = 6.98 \cdot 10^9\ s^{-2}$.

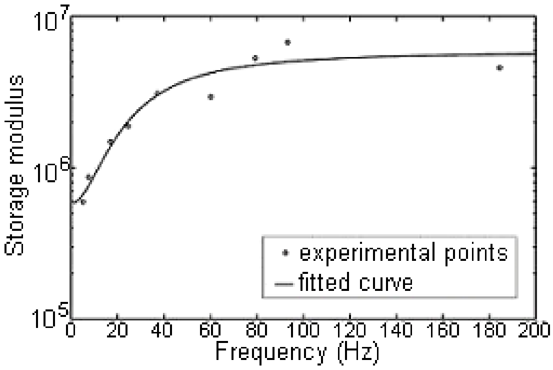

Figure 6: Fitted curve for storage modulus.

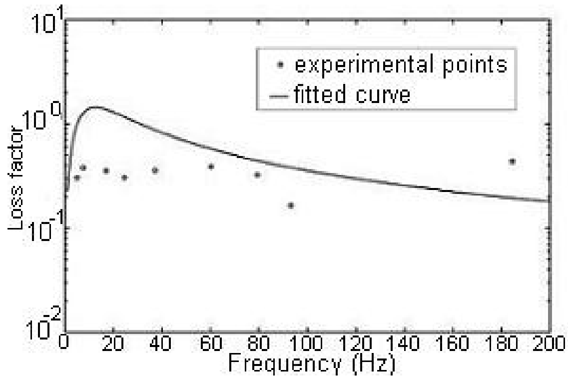

Figure 7: Fitted curve for the loss factor.

The adopted GHM parameters produce a good adjustment for E', over-estimating η for low frequencies and underestimating η for high frequencies. Obviously, it is possible to optimize the solution for both dynamic characteristics, but it is not the focus of this work (Barbosa et al., 2000).

3. The sandwich viscoelastic model

The proposed sandwich viscoelastic model is presented in Figure 8. It is composed by a combination of seven finite elements: two elastic beam elements; one quadrilateral linear viscoelastic plane stress element; and four connection elements. The model has 24 physical dofs (q_1 to q_{24}, numbered from 1 to 24), and 5 dissipation variables (z_1 to z_5 numbered from 25 to 29). The dissipation variable directions plotted in Figure 8 have no physical interpretation. The dimension of the viscoelastic super element matrices is 24 + 5 = 29.

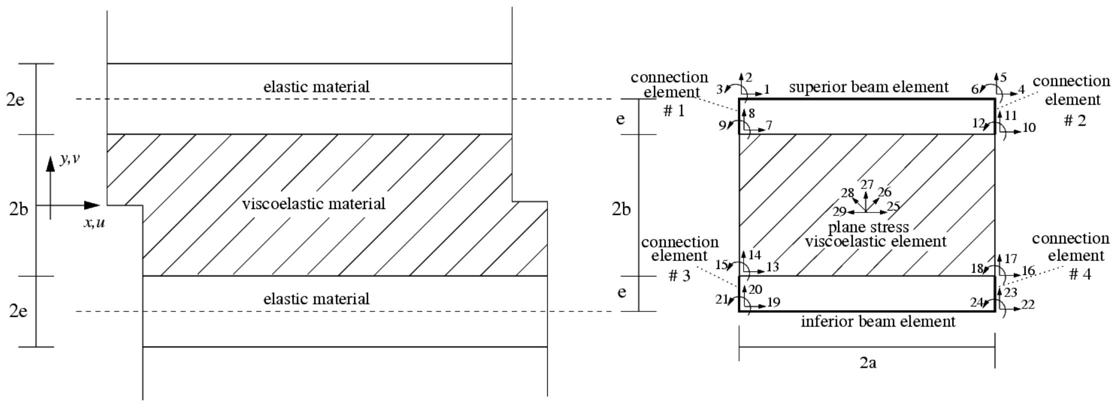

Figure 8: The sandwich finite element.

In order to compute the contribution of each kind of finite element in the composition of the sandwich super element matrices, the problem is decomposed into three parts: a) contribution of the 2 elastic beam elements; b) contribution of the 4 connection elements; c) contribution of the rectangular viscoelastic element;

4.1. Contribution of beam and connection elements

The contribution of these elements for the super element matrices is well known in the literature. It is necessary to observe the connectivity in order to correctly assemble its contributions. Furthermore, concerning connection elements, they only contribute for the super element stiffness matrix.

4.2. Contribution of the quadrilateral viscoelastic element

For the sake of simplicity, the following definition is adopted: for a n-dimensional square matrix $\mathbf{H}$; a k and a p-dimensional vectors $\mathbf{l}$ and $\mathbf{c}$, respectively, where $1 \le k; p \le n$, $\mathbf{H}_{\mathbf{l},\mathbf{c}}$ is defined as a sub-matrix of $\mathbf{H}$ with lines $\mathbf{l}$ and columns $\mathbf{c}$.

The quadrilateral linear viscoelastic plane-stress part of the sandwich element is obtained from a linear plane-stress elastic element presented in Figure 9, whose displacement field is defined as linear contributions for the super element matrix $\mathbf{K}$ as shown in Eqs. (12), (13) and (14).

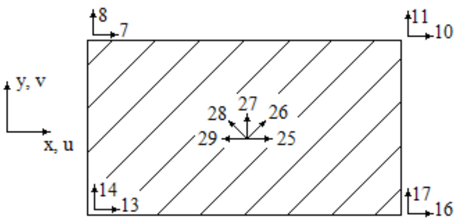

Figure 9: The quadrilateral linear plane stress viscoelastic element.

$$\mathbf{K}_{\mathbf{l}_1,\mathbf{c}_1} = \begin{bmatrix} k_1^e & k_2^e & k_3^e & k_4^e & -\frac{k_1^e}{2} & -k_2^e & k_5^e & -k_4^e \\ k_2^e & k_6^e & -k_4^e & k_7^e & -k_2^e & -\frac{k_6^e}{2} & k_4^e & k_8^e \\ k_3^e & -k_4^e & k_1^e & -k_2^e & k_5^e & k_4^e & -\frac{k_1^e}{2} & k_2^e \\ k_4^e & k_7^e & -k_2^e & k_6^e & -k_4^e & k_8^e & k_2^e & -\frac{k_6^e}{2} \\ -\frac{k_1^e}{2} & -k_2^e & k_5^e & -k_4^e & k_1^e & k_2^e & k_3^e & k_4^e \\ -k_2^e & -\frac{k_6^e}{2} & k_4^e & k_8^e & k_2^e & k_6^e & -k_4^e & k_7^e \\ k_5^e & k_4^e & -\frac{k_1^e}{2} & k_2^e & k_3^e & -k_4^e & k_1^e & -k_2^e \\ -k_4^e & k_8^e & k_2^e & -\frac{k_6^e}{2} & k_4^e & k_7^e & -k_2^e & k_6^e \end{bmatrix} \quad (12)$$

where: $\mathbf{l}_1 = \mathbf{c}_1 = [10 \quad 11 \quad 7 \quad 8 \quad 13 \quad 14 \quad 16 \quad 17]$; $k_1^e = \dfrac{r^2 d_1 + d_3}{3r}$; $k_2^e = \dfrac{d_2 + d_3}{4}$; $k_3^e = -\dfrac{2r^2 d_1 - d_3}{6r}$; $k_4^e = \dfrac{d_2 - d_3}{4}$; $k_5^e = \dfrac{r^2 d_1 - 2d_3}{6r}$; $k_6^e = \dfrac{r^2 d_3 + d_1}{3r}$; $k_7^e = -\dfrac{2r^2 d_3 - d_1}{6r}$; $k_8^e = \dfrac{r^2 d_3 - 2d_1}{6r}$; $d_1 = \dfrac{1}{1-\nu^2}$; $d_2 = \dfrac{1-\nu}{2(1-\nu^2)}$; $d_3 = \dfrac{\nu}{1-\nu^2}$; ν is the Poisson ration of the viscoelastic material; $r = b/a$, $2a$, $2b$ and t are, respectively, the length, height and thickness of the quadrilateral element.

$$\mathbf{K}_{\mathbf{l}_2,\mathbf{c}_2} = diag\{\alpha, \alpha, \alpha, \alpha, \alpha\} \quad (13)$$

where: $\mathbf{l}_2 = \mathbf{c}_2 = [25 \quad 26 \quad 27 \quad 28 \quad 29]$, and

$$\mathbf{K}_{\mathbf{l}_3,\mathbf{c}_3} = \begin{bmatrix} +7.3098e-01 & -3.7222e+01 & +0.0000e+00 & -2.1556e+01 & +2.8246e+00 \\ -6.0783e+01 & +1.7867e+00 & -3.5108e+01 & +0.0000e+00 & +3.3968e-02 \\ -7.3098e-01 & -3.7222e+01 & +0.0000e+00 & +2.1556e+01 & -2.8246e+00 \\ -6.0783e+01 & -1.7867e+00 & +3.5108e+01 & +0.0000e+00 & +3.3968e-02 \\ +7.3098e-01 & +3.7222e+01 & +0.0000e+00 & +2.1556e+01 & +2.8246e+00 \\ +6.0783e+01 & +1.7867e+00 & +3.5108e+01 & +0.0000e+00 & -3.3968e-02 \\ -7.3098e-01 & +3.7222e+01 & +0.0000e+00 & -2.1556e+01 & -2.8246e+00 \\ +6.0783e+01 & -1.7867e+00 & -3.5108e+01 & +0.0000e+00 & -3.3968e-02 \end{bmatrix} \quad (14)$$

where: $\mathbf{l}_3 = [10 \quad 11 \quad 7 \quad 8 \quad 13 \quad 14 \quad 16 \quad 17]$ and $\mathbf{c}_3 = [25 \quad 26 \quad 27 \quad 28 \quad 29]$. Due to the eigenvalue problem involved in the solution of the viscoelastic stiffness matrix, numerical values where presented in Eq. (14), obtained for $r = 4.8000e-02$, thickness = 24 mm and Poisson's ratio = 0.25.

The quadrilateral linear plane-stress viscoelastic element contribution for the super element matrices $\mathbf{M}$ and $\mathbf{C}$ is presented in Eqs. (15) and (16), respectively.

$$\mathbf{M}_{\mathbf{l},\mathbf{c}} = diag\left\{\mu,\mu,\mu,\mu,\mu,\mu,\mu,\mu,\frac{\alpha}{\delta},\frac{\alpha}{\delta},\frac{\alpha}{\delta},\frac{\alpha}{\delta},\frac{\alpha}{\delta},\right\} \quad (15)$$

$$\mathbf{C}_{\mathbf{l},\mathbf{c}} = diag\left\{0,0,0,0,0,0,0,0,\frac{\alpha\beta}{\delta},\frac{\alpha\beta}{\delta},\frac{\alpha\beta}{\delta},\frac{\alpha\beta}{\delta},\frac{\alpha\beta}{\delta},\right\} \quad (16)$$

where: $\mathbf{l} = \mathbf{c} = [10 \quad 11 \quad 7 \quad 8 \quad 13 \quad 14 \quad 16 \quad 17 \quad 25 \quad 26 \quad 27 \quad 28 \quad 29]$, $\mu = \rho_v abt$ where ρ_v is the viscoelastic material density.

It is important to observe that the proposed sandwich FE allows discontinuity in the displacement field between the beams and the quadrilateral viscoelastic element. In this case, the errors inherent to the proposed FE must be investigated through the mesh convergence analysis.

5. Example of numerical application

In this section, a sandwich finite element model of a clumped-free beam obtained with the proposed methodology is analyzed. Free vibration tests are performed and the numerical results are compared to the experimental counterpart.

5.1. The sandwich beam FE model

The dynamic behavior of the 100 cm long sandwich beam (experimentally tested in section 3) was computationally modeled with the sandwich element proposed in this work.

The FE model was adopted after the convergence analysis. Results for a free vibration test with impact load applied in models with 6, 12, 24 and 48 sandwich super elements were analyzed and it was verified, by regarding Figure 10, that results for 24 and 48 are practically coincident. Due to this fact, the adopted model has 24 super elements it is presented in Figure 11.

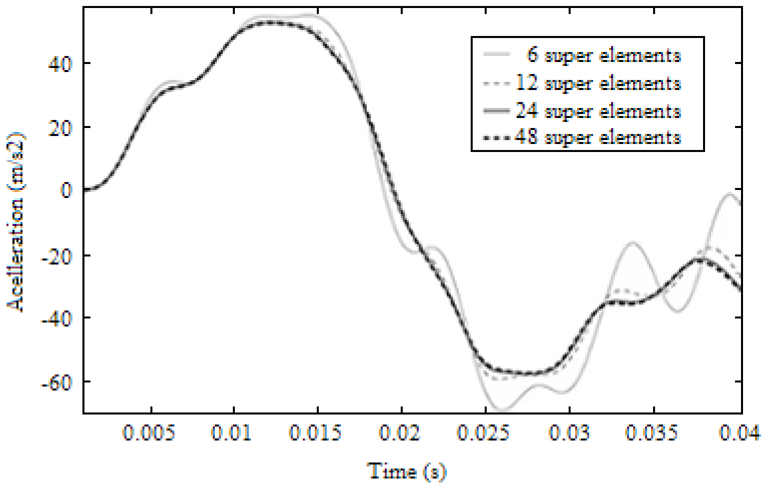

Figure 10: Convergence analysis of the FE model.

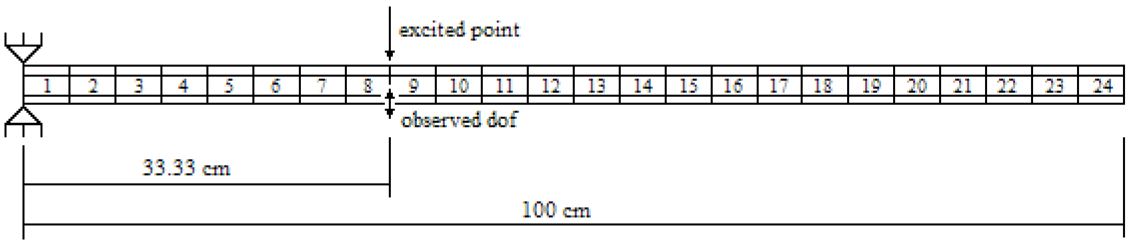

Figure 11: The adopted FE model.

Physical and geometric characteristics of the model are presented in Tables 3 and 4, respectively. The viscoelastic GHM parameters used in the computational model were determined as described in section 3.

	Aluminum	Viscoelastic material	Material of the connection elements
Young’s modulus (GPa)	68.70	Variable	6870.00
Density (kg/m³)	2690	795	0
Poisson’s ratio	Not used	0.25	Not used

Table 3: Summary of material properties.

	Superior and inferior beam elements	Quadrilateral viscoelastic elements	connection elements
Cross section width (mm)	24	24	24
Cross section height (mm)	3	2	3

Table 4: Summary of geometrical properties.

The super element finite element matrices may be calculated using equations of section 4. For the 24 super elements used in the discretization, it implies 332 physical dof and 120 dissipation variables.

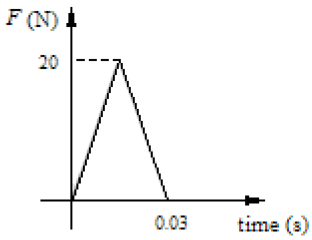

Figure 12: The excitation function.

The set of 452 differential equations was integrated using Newmark method with 8333 time steps of 0.00012 s, consuming 95% of the total CPU processing time which reached 12,35 s in a Matlab implementation on a Pentium IV 2.8 GHz.

The time domain responses were filtered with a low-pass filter in 200 Hz, as it was made in the experimental tests.

The adopted sandwich beam model was submitted to an excitation function presented in Figure 12 which simulates the hammer impact of the experimental test.

5.2. Comparison between numerical and experimental results

Figure 13 shows a comparison between the experimental and the numerical time responses, indicating an adequate correlation.

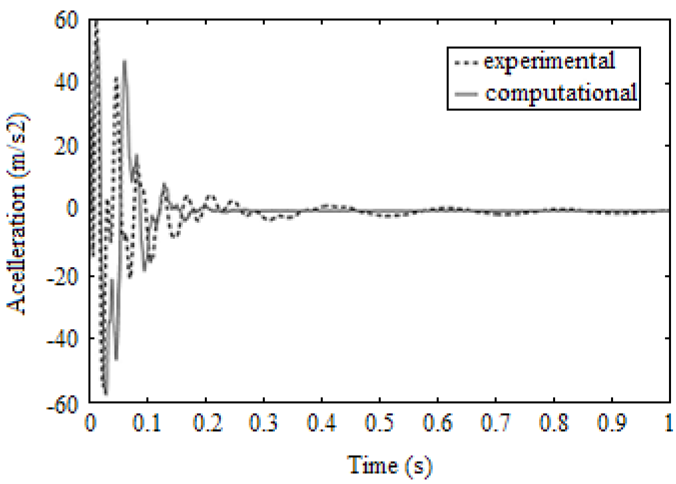

Figure 13: Comparisons between numerical and experimental results.

The differences between numerical and experimental results are in agreement with the adopted viscoelastic model. It is possible to visually verify in Figure 13 that low frequency oscillations of the numerical model tends to zero faster than the experimental results. Whilst, high frequency oscillations of the numerical model tends to zero slower than the experimental results. It is due to the over-estimation and underestimation of the loss factor in low and high frequencies, respectively. On the other hand, the acceleration level of the model is very close to the experimental counterpart, probably due to the good agreement between experimental data and the fitted curve for the storage modulus.

In a qualitative point of view, these results are almost equivalent, considering that the acceleration level in the time interval 0 to 0.1 second is practically the same and also that the acceleration level past 0.3 second is practically negligible for both analysis.

These results indicate the good performance of the proposed FE model.

6. Conclusions

A GHM based sandwich FE model was presented in this work. All the element matrices were developed and presented as well as the experimental procedures necessary to evaluate GHM parameters. A numerical model using the proposed FE was dynamically tested and the obtained results were compared with experimental results counterpart, showing good agreement.

7. References

Asmussen JC. Modal Analysis Based on the Random Decrement Technique - Application to Civil Engineering Structures. PhD thesis, Aalborg University, Danemark, 1998.
Barbosa FS. Computational modeling of structures with damper viscoelastic layers (in Portuguese). PhD thesis COPPE/UFRJ - Federal University of Rio de Janeiro, Brazil, 2000.
Barbosa FS, Battista, RC. A time and frequency domain modeling of structures with damper viscoelastic layers (in Portuguese). Punta del Este, Uruguay, proceedings (CDROM) of XXIX Jornadas Sudamericanas de Ingenierí Estructural 2000.
Barbosa FS, Lemonge ACC, Toledo EM. Parametric analysis of viscoelastic materials via parallel genetic algorithms. Rio de Janeiro, Brazil, proceedings (CDROM) of XXI Iberian Latin-American Congress on Computational Method in Engineering 2000, in Portuguese.
Barrett KE, Gotts, AC. Finite element analysis of a compressible dynamic viscoelastic sphere using FFT. Computers & Structures 2002; 80:1615-1625.
Battista RC, Batista EM, Pfeil MS. Experimental tests on a prototype scale model of the slender sandwich concrete-viscoelastic-steel deck for rehabilitation of the Rio-Niterói bridge, in Portuguese. Rio de Janeiro, Brazil. Contract Report COPPETEC ET-150771 with Ponte S.A. - Concessionaire of the Rio-Niterói Bridge 1998.
Battista RC, Pfeil MS. Strengthening fatigue cracked orthotropic decks with composite layers. Rio de Janeiro, Brazil. proceedings of Intern. Assoc. for Bridge and Structural Engineering - IABSE Symposium 1999; II:853-860.
Beijer JGJ, Spoormaker JL. Solution strategies for FEM analysis with nonlinear viscoelastic polymers. Computers & Structures 2002; 80:1213-1229.
Cremona C, Barbosa FS, Alvandi A. Modal identification under ambient excitation: Application to bridge monitoring. Mécanique & Industries 2003; 4:259-271
Ewins DJ. Modal testing: theory, practice and application. 2000.
Faisca RG. Characterization of viscoelastic materials as structural dampers, in portuguese. M.Sc. thesis COPPE/UFRJ - Federal University of Rio de Janeiro, Brazil, 1998.
Golla DF, Hughes PC. Dynamics of viscoelastic structures - a time-domain,finite element formulation. Journal of Applied Mechanics 1985; 52:897-906.
Kaliske M, Rothert H. Formulation an implementation of three-dimensional viscoelasticity at small and finite strains. Computational Mechanics 1997; 19:228-239.
Kervin Jr EM. Damping of Flexural Waves by a Constrained Viscoelastic Layer". Journal of the Acoustical Society of America 1959; 31:952-962.
Kyowa Electronic Instruments Co. Ltd. Accelerometers user guide 2007. http://www.kyowa-ei.co.jp/english/index e.htm.
Lynx Tecnologia Eletrônica. ADS2000 User guide 2007; http://www.lynxtec.com.br/
Mahmoodi P. Structural dampers. ASCE - Journal of Structural Division 1969; 95(ST8):1661-1672.
Mesquita AD, Coda HB. New methodology for the treatment of two dimensional viscoelastic coupling problems. Computer methods in applied mechanics and engineering 2003; 192:1911-1927.
Nashif AD, Jones DIG, Henderson JP. Vibration Damping. John Wiley & Sons.USA 1985.

Oberst H, Frankenfeld K. Uber die Dampfung der Biegeschwingungen dunner Bleche durch festhaftende Belage. Acustica 1952; 2:181-194.
Qian C, Demao Z. Vibrational analysis theory and application to elastic-viscoelastic composite structure. Computer & Structures 1990; 37(4):585-595.
Ross D, Ungar EE, Kervin Jr EM. Damping of Plate Flexural Vibrations by Means of Viscoelastic Laminate. Structural Damping ASME 1959; 49-88.
Samali B, Kwok KCS. Use of Viscoelastic Dampers in Reducing Wind- and Earthquake-induced Motion of Building Structures. Engineering Structure 1995; 17(9): 639-654.
Vasconcelos RP. Dynamic structural control via viscoelastic mechanisms, in Portuguese. PhD thesis COPPE/UFRJ - Federal University of Rio de Janeiro, Brazil, 2003.
Vasconcelos RP. Modeling viscoelastic laminated structures via weighing damping modal superposition technique. Ouro Preto, Brazil, proceedings (CDROM) of XXIV Iberian Latin-American Congress on Computational Method in Engineering 2003, in Portuguese.
Yi S, Shih FL, Ying M. Finite element analysis of composite structures with smart constrained layer damping. Advances in Engineering Software 1998; 29(3-6):265-271.